

# Finite Element Method for Nonlinear Vibration Analysis of Plates

Stanislav Stoykov and Svetozar Margenov

**Abstract** Plates are structures which have wide applications among engineering constructions. The knowledge of the dynamical behavior of the plates is important for their design and maintenance. The dynamical response of the plate can change significantly due to the nonlinear terms at the equation of motion which become essential in the presence of large displacements. The current work presents numerical methods for investigating the dynamical behavior of plates with complex geometry. The equation of motion of the plate is derived by the classical plate theory and geometrical nonlinear terms are included. It is discretized by the finite element method and periodic responses are obtained by shooting method. Next point from the frequency-response curve is obtained by the sequential continuation method. The potential of the methods is demonstrated on rectangular plate with hole. The main branch along the fundamental mode is presented and the corresponding time responses and shapes of vibration are shown.

## 1 Introduction

Plates are thin structures and due to strong external loads their displacements can become large. Linear theories are not appropriate for modeling large displacements thus one should include geometrical nonlinear terms at the equation of motion for obtaining more accurate and reliable results. The nonlinearities can change drastically

---

S. Stoykov (✉) · S. Margenov  
Institute of Information and Communication Technologies,  
Bulgarian Academy of Sciences, Acad. G. Bonchev Str., bl. 25A,  
1113 Sofia, Bulgaria  
e-mail: stoykov@parallel.bas.bg

S. Margenov  
e-mail: margenov@parallel.bas.bg

the behavior of the system, thus additional tools for analyzing such systems need to be used. The aim of the work is to present efficient numerical methods for analyzing nonlinear dynamical systems which arise from space discretization of elastic plates with complex geometry.

The equation of motion of the plate is derived assuming classical plate theory and including geometrically nonlinear terms. It is discretized into a system of ordinary differential equations (ODE) by the finite element method. The variation of the periodic steady-state responses with the excitation frequency are of interest for the dynamical analysis, thus periodic responses due to external harmonic excitations are obtained by shooting method. Newmark's time integration scheme is used for solving the ODE in time domain. The resulting nonlinear algebraic system is solved by Newton's method. Prediction for the next point from the frequency-response curve is defined by the sequential continuation method. The process involves simultaneously solvers for sparse and dense matrices. The complete process of computing the frequency-response curve becomes computationally slow and burdensome when the resulting ODE system is large. A suitable parallel implementation used for beams and three-dimensional structures in [6] is also applied here.

## 2 Equation of Motion of Plates

The nonlinear equation of motion of plate is derived in Cartesian coordinate system assuming classical plate theory, also known as Kirchoff's hypotheses. Only transverse displacements are considered on the middle plane. Kirchoff's hypotheses states that stresses in the direction normal to the plate middle surface are negligible and strains vary linearly within the plate thickness [5].

Assuming Kirchoff's hypotheses, the in-plane displacements  $u(x, y, z, t)$  and  $v(x, y, z, t)$  and the out-of-plane displacement  $w(x, y, z, t)$  are expressed by the out-of-plane displacement on the middle plane  $w_0(x, y, t)$ :

$$\begin{aligned} u(x, y, z, t) &= -z \frac{\partial w_0(x, y, t)}{\partial x}, \\ v(x, y, z, t) &= -z \frac{\partial w_0(x, y, t)}{\partial y}, \\ w(x, y, z, t) &= w_0(x, y, t). \end{aligned} \tag{1}$$

The middle plane is defined for  $z = 0$ . Using the nonlinear strain-displacement relations from Green's strain tensor and assuming that  $\varepsilon_z$ ,  $\gamma_{xz}$  and  $\gamma_{yz}$  are negligible, i.e.  $\varepsilon_z = \gamma_{xz} = \gamma_{yz} = 0$ , the following expressions are obtained:

$$\begin{aligned}
\varepsilon_x &= \frac{\partial u}{\partial x} + \frac{1}{2} \left( \frac{\partial w}{\partial x} \right)^2 = -z \frac{\partial^2 w_0}{\partial x^2} + \frac{1}{2} \left( \frac{\partial w_0}{\partial x} \right)^2, \\
\varepsilon_y &= \frac{\partial v}{\partial y} + \frac{1}{2} \left( \frac{\partial w}{\partial y} \right)^2 = -z \frac{\partial^2 w_0}{\partial y^2} + \frac{1}{2} \left( \frac{\partial w_0}{\partial y} \right)^2, \\
\gamma_{xy} &= \frac{\partial u}{\partial y} + \frac{\partial v}{\partial x} + \frac{\partial w}{\partial x} \frac{\partial w}{\partial y} = -2z \frac{\partial^2 w_0}{\partial x \partial y} + \frac{\partial w_0}{\partial x} \frac{\partial w_0}{\partial y}.
\end{aligned} \tag{2}$$

The stresses are related to the strains by the constitutive relations written in reduced form. For isotropic materials this relation is given by:

$$\begin{Bmatrix} \sigma_x \\ \sigma_y \\ \tau_{xy} \end{Bmatrix} = \frac{E}{1-\nu^2} \begin{bmatrix} 1 & \nu & 0 \\ \nu & 1 & 0 \\ 0 & 0 & \frac{1-\nu}{2} \end{bmatrix} \begin{Bmatrix} \varepsilon_x \\ \varepsilon_y \\ \gamma_{xy} \end{Bmatrix}, \tag{3}$$

where  $E$  is the Young's modulus and  $\nu$  is the Poisson's ratio. The equation of motion is derived by the Hamilton's principle:

$$\int_{t_1}^{t_2} (\delta T - \delta \Pi + \delta W) dt = 0, \tag{4}$$

where  $T$  is the kinetic energy,  $\Pi$  is the potential energy and  $W$  is the work done by external loads:

$$T = \rho \int_V (u\ddot{u} + v\ddot{v} + w\ddot{w}) dV, \tag{5}$$

$$\Pi = \int_V (\varepsilon_x \sigma_x + \varepsilon_y \sigma_y + \gamma_{xy} \tau_{xy}) dV, \tag{6}$$

$$W = \int_V q(x, y, t) w dV, \tag{7}$$

where by double dot is denoted the second derivative with respect to time,  $V$  is the volume of the plate,  $\rho$  is the density and  $q(x, y, t)$  is the applied external load in transverse direction. The equation of motion is obtained in the following form:

$$\begin{aligned}
&\rho h \frac{\partial^2 w_0}{\partial t^2} + \frac{Eh^3}{12(1-\nu^2)} \left( \frac{\partial^4 w_0}{\partial x^4} + 2 \frac{\partial^4 w_0}{\partial x^2 \partial y^2} + \frac{\partial^4 w_0}{\partial y^4} \right) \\
&= q + \frac{\rho h^3}{12} \frac{\partial^2}{\partial t^2} \left( \frac{\partial^2 w_0}{\partial x^2} + \frac{\partial^2 w_0}{\partial y^2} \right) + N_x \frac{\partial^2 w_0}{\partial x^2} + 2N_{xy} \frac{\partial^2 w_0}{\partial x \partial y} + N_y \frac{\partial^2 w_0}{\partial y^2},
\end{aligned} \tag{8}$$

where  $h$  is the thickness and  $N_x$ ,  $N_y$  and  $N_{xy}$  are the stress resultants given by:

$$\begin{aligned} N_x &= \frac{Eh}{1-\nu^2} \left( \frac{1}{2} \left( \frac{\partial w_0}{\partial x} \right)^2 + \frac{\nu}{2} \left( \frac{\partial w_0}{\partial y} \right)^2 \right), \\ N_y &= \frac{Eh}{1-\nu^2} \left( \frac{1}{2} \left( \frac{\partial w_0}{\partial y} \right)^2 + \frac{\nu}{2} \left( \frac{\partial w_0}{\partial x} \right)^2 \right), \\ N_{xy} &= \frac{Eh}{2(1+\nu)} \left( \frac{\partial w_0}{\partial x} \frac{\partial w_0}{\partial y} \right). \end{aligned} \quad (9)$$

In the current work are considered simply-supported boundary conditions. The essential boundary condition, which is imposed in the space of admissible functions, is given by:

$$w_0(x, y, t) = 0. \quad (10)$$

The natural boundary condition is related with the second derivatives of the transverse displacement  $w_0$ . It is not imposed in the finite element model, but it is automatically satisfied. Details about the derivation of the equation of motion can be found, for example in [4].

### 3 Finite Element Method and Computation of Periodic Responses

The partial differential Eq. (8) is discretized by the finite element method [7]. A mesh of rectangular elements is used. The reference finite element is square element with local coordinates denoted by  $\xi$  and  $\eta \in [-1, 1]$ . The element has 4 nodes, each node is considered to have 4 degrees of freedom (DOF), i.e.  $w_0$ ,  $\frac{\partial w_0}{\partial \xi}$ ,  $\frac{\partial w_0}{\partial \eta}$  and  $\frac{\partial^2 w_0}{\partial \xi \partial \eta}$ . Hence, each element has 16 DOF. The transverse displacement  $w_0$  is approximated by the shape functions within each element by:

$$w^e(\xi, \eta, t) = \sum_{i=1}^{16} q_i(t) \psi_i(\xi, \eta), \quad (11)$$

where  $\psi_i(\xi, \eta)$ ,  $i = 1, \dots, 16$  are the shape functions and  $q_i(t)$  are the local unknowns (DOF). The finite element is conforming, the FEM space is  $\mathcal{V}_h \subset \mathcal{H}_2(\Omega)$ .

The equation of motion is written in variational form and application by parts is applied. Assuming the approximation (11) for the transverse displacement  $w_0$ , and

using the same expression for the test functions, a system of nonlinear ordinary differential equations of the following type is obtained:

$$\mathbf{M}\ddot{\mathbf{q}}(t) + \mathbf{C}\dot{\mathbf{q}}(t) + \mathbf{K}_L\mathbf{q}(t) + \mathbf{K}_{NL}(\mathbf{q}(t))\mathbf{q}(t) = \mathbf{F}(t), \quad (12)$$

where  $\mathbf{M}$  represents the mass matrix,  $\mathbf{K}_L$  represents the stiffness matrix of constant terms,  $\mathbf{K}_{NL}(\mathbf{q}(t))$  represents the stiffness matrix that depends on the global vector of unknowns  $\mathbf{q}(t)$ ,  $\mathbf{F}(t)$  is the global vector of external forces and  $\mathbf{C}$  is the damping matrix. Stiffness proportional damping is considered in the model, hence the damping matrix is expressed as  $\mathbf{C} = \alpha\mathbf{K}_L$ , where  $\alpha$  is the factor of proportionality.

The external force  $\mathbf{F}(t)$  is assumed to be harmonic:

$$\mathbf{F}(t) = \mathbf{A}\cos(\omega t), \quad (13)$$

where  $\mathbf{A}$  is the force vector and  $\omega$  is the excitation frequency.

Equation (12) is solved in frequency domain where each point from the frequency-response curve presents a periodic solution. Shooting method is used to compute the periodic responses. The method consists of iterative correction of the initial conditions that lead to periodic solution.

Of interest are the initial conditions  $\mathbf{q}(0) = \mathbf{q}_0$  and  $\dot{\mathbf{q}}(0) = \dot{\mathbf{q}}_0$  which satisfy the equations:

$$\mathbf{q}(T, \mathbf{q}_0, \dot{\mathbf{q}}_0) = \mathbf{q}_0, \quad (14)$$

$$\dot{\mathbf{q}}(T, \mathbf{q}_0, \dot{\mathbf{q}}_0) = \dot{\mathbf{q}}_0, \quad (15)$$

where  $T$  is the minimal period of vibration which is determined from the excitation frequency,  $\mathbf{q}(T, \mathbf{q}_0, \dot{\mathbf{q}}_0)$  and  $\dot{\mathbf{q}}(T, \mathbf{q}_0, \dot{\mathbf{q}}_0)$  present the response and velocity of the equation of motion (12) at time  $T$  due to initial conditions  $\mathbf{q}_0$  and  $\dot{\mathbf{q}}_0$ . The initial conditions are also written in the response and velocity, in order to outline the dependence of the solution on the initial conditions.

The method finds corrections of the initial conditions  $\mathbf{q}_0$  and  $\dot{\mathbf{q}}_0$  in such a way that the response of the system with the corrected initial conditions performs periodic steady-state vibration. I.e. of interest is to find  $\delta\mathbf{q}_0$  and  $\delta\dot{\mathbf{q}}_0$  such that

$$\begin{aligned} \|\mathbf{q}(T, \mathbf{q}_0 + \delta\mathbf{q}_0, \dot{\mathbf{q}}_0 + \delta\dot{\mathbf{q}}_0) - \mathbf{q}_0 - \delta\mathbf{q}_0\| &< \epsilon, \\ \|\dot{\mathbf{q}}(T, \mathbf{q}_0 + \delta\mathbf{q}_0, \dot{\mathbf{q}}_0 + \delta\dot{\mathbf{q}}_0) - \dot{\mathbf{q}}_0 - \delta\dot{\mathbf{q}}_0\| &< \epsilon, \end{aligned} \quad (16)$$

for some small  $\epsilon$ .

The corrections  $\delta\mathbf{q}_0$  and  $\delta\dot{\mathbf{q}}_0$  are obtained by solving the following linear system:

$$\begin{bmatrix} \mathbf{Q}_d(T) - \mathbf{I} & \mathbf{Q}_v \\ \dot{\mathbf{Q}}_d(T) & \dot{\mathbf{Q}}_v(T) - \mathbf{I} \end{bmatrix} \begin{Bmatrix} \delta\mathbf{q}_0 \\ \delta\dot{\mathbf{q}}_0 \end{Bmatrix} = \begin{Bmatrix} \mathbf{q}_0 - \mathbf{q}(T, \mathbf{q}_0, \dot{\mathbf{q}}_0) \\ \dot{\mathbf{q}}_0 - \dot{\mathbf{q}}(T, \mathbf{q}_0, \dot{\mathbf{q}}_0) \end{Bmatrix}. \quad (17)$$

The matrix in Eq. (17) is obtained by solving another initial value problem, i.e.  $\mathbf{Q}_d(T)$  and  $\dot{\mathbf{Q}}_d(T)$  are solutions at time  $T$  of the system:

$$\mathbf{M}\ddot{\mathbf{Q}}(t) + \mathbf{C}\dot{\mathbf{Q}}(t) + \mathbf{K}_L\mathbf{Q}(t) + \mathbf{J}(\mathbf{q}(t))\mathbf{Q}(t) = \mathbf{0} \quad (18)$$

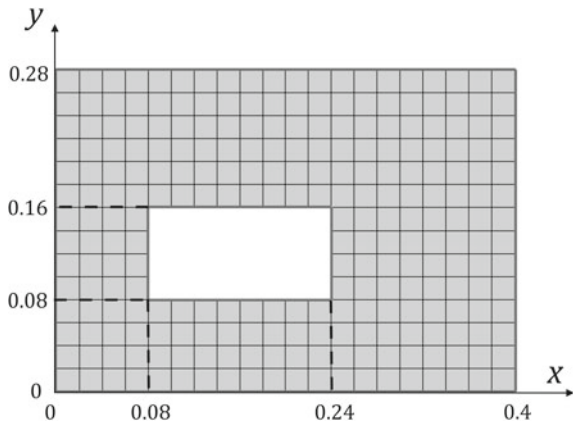
due to initial conditions  $\mathbf{Q}_d(0) = \mathbf{I}$  and  $\dot{\mathbf{Q}}_d(0) = \mathbf{0}$ .  $\mathbf{Q}_v(T)$  and  $\dot{\mathbf{Q}}_v(T)$  are solutions at time  $T$  of the system (18) due to initial conditions  $\mathbf{Q}_v(0) = \mathbf{0}$  and  $\dot{\mathbf{Q}}_v(0) = \mathbf{I}$ .  $\mathbf{J}(\mathbf{q}(t))$  is the Jacobian of the nonlinear terms of the equation of motion (12), i.e.

$$\mathbf{J}(\mathbf{q}(t)) = \frac{\partial \mathbf{K}_{NL}(\mathbf{q}(t))\mathbf{q}(t)}{\partial \mathbf{q}(t)}. \quad (19)$$

The shooting method requires time integration scheme for obtaining the responses of Eqs. (12) and (18) from time 0 to  $T$ . Newmark's method is used for the time integration. Newton's method is used for solving the resulting nonlinear algebraic system of Eq. (12) after application of Newmark's method. Equation (18) presents linear system of ODE, thus Newton's method is applied only to Eq. (12). Next point from the frequency-response curve is computed by increasing the excitation frequency and repeating the shooting procedure. This parametric analysis is known as sequential continuation method.

In the cases of plates with complex geometries (Fig. 1), the necessity of obtaining sufficiently accurate results requires the usage of enough elements. The resulting system of ODE (12) becomes large and the process of computing periodic responses and frequency-response curves becomes computationally burdensome. The parallel implementation of the shooting method, presented in [6] is also applied here. It consists of efficient parallel algorithms for solving large systems of sparse and dense matrices. UMFPACK library [2], which is a direct solver, is used for solving the sparse systems which result from the application of Newmark's method to systems (12) and (18). ScaLAPACK [1] library, which is library of high-performance linear algebra routines for parallel distributed memory machines, is used for solving the dense system (17).

**Fig. 1** Plate with complex geometry and mesh of quadratic finite elements



4 Numerical Tests

4.1 Linear Free Vibration

The developed finite element model is validated by comparing the natural frequencies of rectangular plate with analytical solutions. Rectangular plate with dimensions:  $a = 0.3$  m,  $b = 0.6$  m and thickness  $h = 0.001$  m is considered. The material is assumed to be isotropic with material properties (Aluminum):  $E = 70$  GPa (Young modulus),  $\rho = 2778$  kg/m<sup>3</sup> (density) and  $\nu = 0.3$  (Poisson’s ratio). The results are presented in Table 1. Three different meshes are used in order to investigate the convergence of the FEM. Meshes with rectangular elements of sizes  $\Delta h = 0.05$  m,  $\Delta h = 0.025$  m and  $\Delta h = 0.0125$  m are considered. Figure 2 shows the convergence rates of the natural frequencies. The results correspond to the theoretical estimates and confirm that the FEM model is implemented correctly. The theoretical evaluation of the error of the natural frequencies is  $O(\Delta h^4)$  [3], which is also obtained by the implemented FEM (Fig. 2).

Further to investigate the dynamical behavior of plates with complex geometry, a model of rectangular plate with whole is generated. The plate and its dimensions are presented in Fig. 1, the thickness is  $h = 0.001$  m and the same material properties are assumed (Aluminum). The natural frequencies of the plate are presented in Table 2 and first four mode shapes are presented in Fig. 3.

**Table 1** Comparison of the natural frequencies (rad/s) of FEM model and analytical solutions— $\omega_{mn} = \pi^2[(\frac{m}{a})^2 + (\frac{n}{b})^2]\sqrt{\frac{D}{\rho h}}$ ,  $D = \frac{Eh^3}{12(1-\nu^2)}$

Mode	FEM, 364 DOF	FEM, 1300 DOF	FEM, 4900 DOF	Analytical
1	208.2338	208.2283	208.2279	208.2279
2	333.1668	333.1650	333.1646	333.1646
3	541.4399	541.3965	541.3927	541.3924
4	708.4704	708.0070	707.9768	707.9747
5	833.2874	832.9382	832.9132	832.9114

**Fig. 2** Rates of convergence of first (---), third (· · · · ·) and fourth (···) natural frequencies, ●—computed values

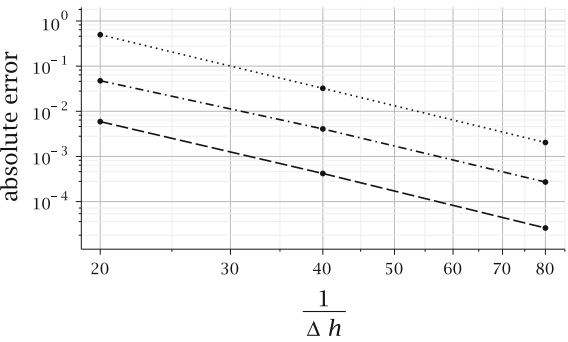


**Table 2** Natural frequencies (rad/s) of plate from Fig. 1

Mode	FEM
1	848.69
2	1214.39
3	1382.06
4	1831.07
5	2249.98
6	2489.70

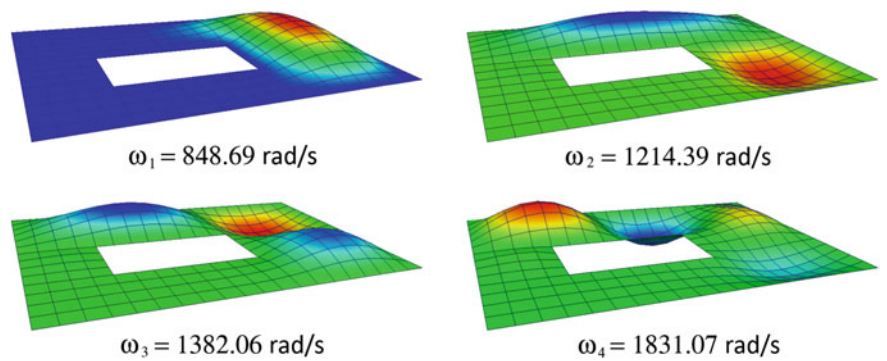
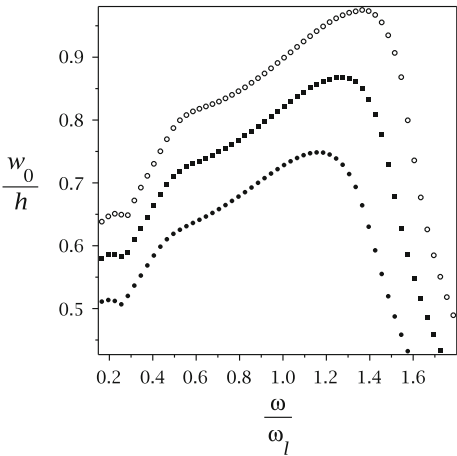


**Fig. 3** First four natural modes of vibration of plate from Fig. 1

4.2 Nonlinear Forced Vibration

Uniformly distributed harmonic loads, with amplitudes of 4, 5 and 6 kN/m<sup>2</sup>, are applied on the plate (Fig. 1) in order to study steady-state forced vibrations. Shooting method is started with small excitation frequency, which is continuously increased. The frequency-response curve is shown in Fig. 4. The amplitude is

**Fig. 4** Frequency-response curves around the first linear mode due to uniformly distributed load of  
○—6 kN/m<sup>2</sup>, ■—5 kN/m<sup>2</sup>, ●—4 kN/m<sup>2</sup>,  $w_0$ —maximum transverse displacement at point  $(x, y) = (0.32, 0.16 \text{ m})$ ,  $h$  thickness,  $\omega/\omega_l$  fundamental dimensionless frequency





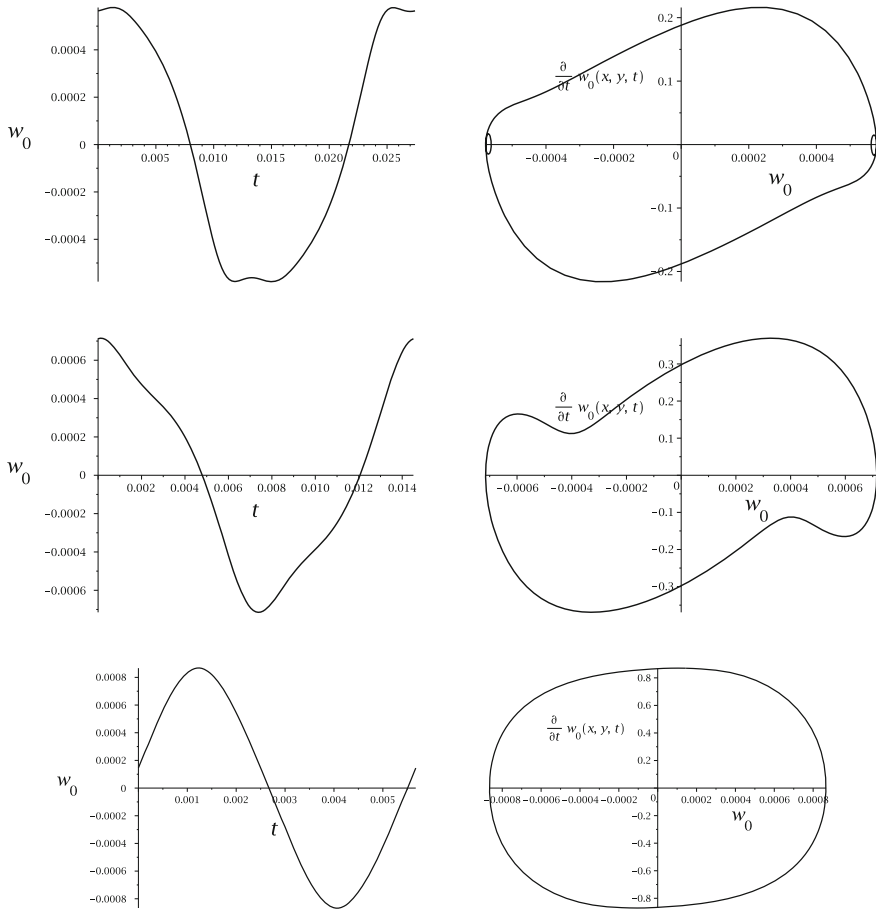


**Fig. 5** Time and phase plots for different excitation frequencies of point  $(x, y) = (0.32 \text{ m}, 0.16 \text{ m})$ , uniformly distributed load of  $5 \text{ kN/m}^2$ , first row  $\omega/\omega_l = 0.27$ , second row  $\omega/\omega_l = 0.5$ , third row  $\omega/\omega_l = 1.3$

measured at point  $(x, y) = (0.32 \text{ m}, 0.16 \text{ m})$  which is the point with maximum displacement on the first linear mode. The figure shows that there is decrease of the amplitude for small values of the excitation frequency and then the amplitude increases for values of the excitation frequency close to the linear mode.

Figure 5 presents time responses and phase plots of the plate for different excitation frequencies. It can be seen from the time response and the phase plot that the third harmonic appears in the response for  $\omega/\omega_l = 0.27$ , which is due to a super-harmonic resonance. When the excitation frequency is close to the linear frequency, the first harmonic is dominant and the response is similar to harmonic (Fig. 5,  $\omega/\omega_l = 1.3$ ). Figure 5 confirms that the plate vibrates in nonlinear regime.

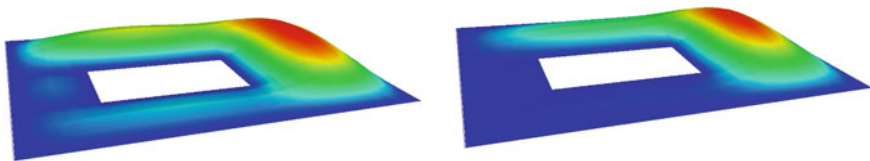


**Fig. 6** Shapes of vibration of the plate for different times,  $\omega = 1.3\omega_l$ , uniformly distributed load of  $5 \text{ kN/m}^2$ , (right)  $t = 0$ , (left)  $t = T/4$

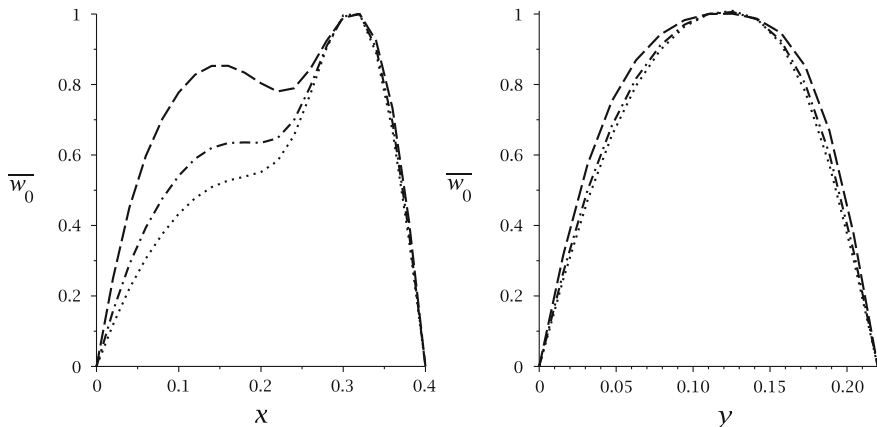


**Fig. 7** Sections of the plate for different times,  $\omega = 1.3\omega_l$ , uniformly distributed load of  $5 \text{ kN/m}^2$ , (right)  $xz$  plane,  $y = 0.2 \text{ m}$ , (left)  $yz$  plane,  $x = 0.32 \text{ m}$ ,  $---$   $t = 0$ ,  $\dots$   $t = T/12$ ,  $-\cdot-\cdot-$   $t = T/4$ ,  $\bar{w}_0$  normalized displacement,  $T$  period of vibration

The shape of vibration changes during the period of vibration, even when the response is close to harmonic. Shapes for different times within one period are shown in Fig. 6, where the amplitude is normalized. The change of the shape can be better seen in Fig. 7, where different sections are presented.

## 5 Conclusion

Numerical methods for computing nonlinear frequency-response curves of plates with complex geometries are presented. The equation of motion is derived by the Hamilton's principle and the classical plate theory and discretized by the finite element method. Geometrical nonlinear terms are included in the model. Periodic responses are computed by the shooting method and next points from the frequency-response curve are defined by the continuation method.

A plate with complex geometry is analyzed in order to investigate the potential of the proposed methods. The main branch of solutions is obtained for loads with

different amplitudes. The effects of the nonlinear terms on the response of the plate and the influence of the excitation frequency are outlined. The proposed numerical methods and the results show that parametric study on the dynamics of complex structures which lead to large-scale dynamical systems can be carried out with appropriate parallel implementation.

**Acknowledgments** This work was supported by the project AComIn “Advanced Computing for Innovations”, grant 316087, funded by the FP7 Capacity Programme.

## References

1. Blackford, L.S., Choi, J., Cleary, A., D’Azevedo, E., Demmel, J., Dhillon, I., Dongarra, J., Hammarling, S., Henry, G., Petitet, A., Stanley, K., Walker, D. Whaley, R.C.: ScaLAPACK users’ guide. Soc. Ind. Appl. Math. (1997)
2. Davis, T.: Algorithm 832: Umfpack, an unsymmetric-pattern multifrontal method. ACM Trans. Math. Softw. **30**(2), 196–199 (2004)
3. Fix, G., Strang, G.: An Analysis of the Finite Element Method. Wellesley-Cambridge Press (2008)
4. Nayfeh, A., Pai, P.: Linear and Nonlinear Structural Mechanics. Wiley (2004)
5. Reddy, J.N.: Mechanics of Laminated Composite Plates and Shells: Theory and Analysis. CRC Press (2004)
6. Stoykov, S., Margenov, S.: Scalable parallel implementation of shooting method for large-scale dynamical systems. application to bridge components. J. Comput. Appl. Math. **293**, 223–231 (2016)
7. Zienkiewicz, O., Taylor, R. Zhu, J.: The Finite Element Method: Its Basis and Fundamentals. Elsevier (2005)

Innovative Approaches and Solutions in Advanced  
Intelligent Systems

Marginov, S.; Angelova, G.; Agre, G. (Eds.)

2016, XIII, 334 p. 143 illus., 101 illus. in color.,

Hardcover

ISBN: 978-3-319-32206-3